

# DESIGNING CYCLOTRONS AND FIXED FIELD ACCELERATORS FROM THEIR ORBITS\*

T. Planche<sup>†</sup>, TRIUMF, Vancouver, Canada

## Abstract

The transverse motion of particles in fixed field accelerators with mid-plane symmetry is entirely determined by the properties of the closed orbits. In this study I exploit this property to produce a variety of isochronous magnetic distributions. All the results presented in this paper are verified using CYCLOPS simulations.

## INTRODUCTION

The transverse tunes of separated sector cyclotrons, and other fixed-field accelerators, can be estimated “on the back of an envelope” using the hard-edge approximation and the concatenation of drift-edge-bend-edge-drift transfer matrices, see for instance Refs. [1–4]. In this paper, I try to go a little further by presenting a way to calculate exactly the transverse tune from the non-hard-edge shape of the closed orbits. The only approximation is that the magnetic field presents a mid-plane symmetry.

The first section is a review of the derivation of the Hamiltonian for linear motion in a magnet with median plane symmetry [5]. The second section is dedicated to derive the relations between the parameters of this Hamiltonian and the geometry of the closed orbit. In the third section, I present examples of isochronous field distributions, and verify my calculations using CYCLOPS. My intention is to show that it is possible to design a cyclotron starting from its orbits, rather than from its field.

In the last section I present an example of application of this method to a non-isochronous fixed field accelerator.

## LINEAR MOTION HAMILTONIAN

Let’s consider a charged particle with mass  $m$  and charge  $q$  travelling in empty space on a closed orbit, under the sole influence of a static magnetic field. Let’s also assume that the closed orbit is contained in a plane. Let  $\rho(s)$  be the curvature of the closed orbit, and  $(x, y, s)$  be the Frenet-Serret coordinates around it. Let the plane of the orbit be the  $y = 0$  plane, and let the magnetic field be everywhere normal to this plane:

$$(\nabla \times \mathbf{A})(0, 0, s) = \begin{pmatrix} 0 \\ B_0(s) \\ 0 \end{pmatrix}, \quad (1)$$

where  $B_0(s) = B(0, 0, s)$ . The vector potential should also satisfy the absence of source along the orbit, which is:

$$(\nabla \times \nabla \times \mathbf{A})(0, 0, s) = \mathbf{0}. \quad (2)$$

Using the definition of the curl operator in the planar Frenet-Serret system:

$$\nabla \times \mathbf{A} = \left( \frac{1}{h} \frac{\partial A_s}{\partial y} - \frac{\partial A_y}{\partial s}, \frac{\partial A_x}{\partial s} - \frac{1}{h} \frac{\partial A_s}{\partial x}, \frac{\partial A_y}{\partial x} - \frac{\partial A_x}{\partial y} \right),$$

$$h = 1 + x/\rho, \quad (3)$$

and considering a vector potential in the form of a truncated power series about the equilibrium orbit [6], we find by inspection that the following vector potential

$$A_x = 0,$$

$$A_y = \frac{\partial B}{\partial s} xy, \quad (4)$$

$$A_s = -\frac{B}{2\rho} (x^2(1+n) + y^2n) - xB,$$

satisfies Eq. (1). It also satisfies Eq. (2) provided that:

$$n = -\frac{\rho}{B_0} \left. \frac{\partial B}{\partial x} \right|_{x=y=0}, \quad (5)$$

which is the standard definition of the magnetic field index.

Let’s now consider the Courant-Snyder Hamiltonian [6]  $H(x, P_x, y, P_y, t, -E; s) =$

$$qA_s - \left( 1 + \frac{x}{\rho} \right) \sqrt{\frac{E^2}{c^2} - m^2c^2 - (P_x - qA_x)^2 - (P_y - qA_y)^2}, \quad (6)$$

where  $E, P_x, P_y$  and  $t$  are, respectively, the particle’s total energy, transverse canonical momenta, and time of flight. For the longitudinal coordinates to be, like the transverse ones, deviations for the reference particle’s coordinates, we proceed to the canonical transformation  $(t, -E) \rightarrow (z = s - \beta ct, \Delta P = \frac{\Delta E}{\beta c})$  using a generating function of the second kind:

$$F_2(t, \Delta P) = \left( \frac{s}{\beta c} - t \right) (E_0 + \beta c \Delta P). \quad (7)$$

where the constants  $\beta c$  and  $E_0$  are, respectively, the reference particle velocity and total energy. The new Hamiltonian is obtained by adding  $\frac{\partial F_2}{\partial s} = \frac{E_0}{\beta c} + \Delta P$  to the old one.<sup>1</sup>

Without changing the dynamics, we scale all the momenta by the constant reference particle’s momentum  $P = \frac{1}{c} \sqrt{E_0^2 - m^2c^4}$ . The scaled momenta become:

$$p_x = P_x/P,$$

$$p_y = P_y/P, \quad (8)$$

$$p_z = \Delta P/P,$$

$$h = H/P.$$

Expanding the resulting Hamiltonian to second order in  $x, y, z, p_x, p_y$ , and  $p_z$ , we find that all first order terms vanish

<sup>1</sup> One can verify that the partial derivative of  $F_2$  w.r.t. the old position  $t$  gives the old momentum  $-E$ . The new position  $z$  is obtained from the partial derivative of  $F_2$  w.r.t. the new momentum  $\Delta P$ .

\* TRIUMF receives funding via a contribution agreement with the National Research Council of Canada.

<sup>†</sup> tplanche@triumf.ca

Content from this work may be used under the terms of the CC BY 3.0 licence (© 2019). Any distribution of this work must maintain attribution to the author(s), title of the work, publisher, and DOI FRB01 354

provided that:

$$\rho = \frac{P}{qB_0}, \quad (9)$$

and

$$\beta = Pc/E_0. \quad (10)$$

In other words, under these two conditions, a particle placed right on the reference orbit will remain on it. Removing the constant terms, which do not contribute to the dynamics, the Hamiltonian becomes:

$$h = \frac{x^2}{2} \frac{1-n}{\rho^2} + \frac{y^2}{2} \frac{n}{\rho^2} + \frac{p_x^2}{2} + \frac{p_y^2}{2} - \frac{p_z x}{\rho} + \frac{p_z^2}{2\gamma^2}, \quad (11)$$

where  $\gamma = \frac{1}{\sqrt{1-\beta^2}}$ .

The equations of motion that derive from this quadratic Hamiltonian can be written in matrix form as:

$$\mathbf{X}' = \mathbf{F}\mathbf{X}, \quad (12)$$

where a prime ' denotes a total derivative w.r.t. the independent variable  $s$ . The matrix  $\mathbf{F}$ :

$$\mathbf{F} = \begin{pmatrix} 0 & 1 & 0 & 0 & 0 & 0 \\ \frac{n(s)-1}{\rho(s)^2} & 0 & 0 & 0 & 0 & \frac{1}{\rho(s)} \\ 0 & 0 & 0 & 1 & 0 & 0 \\ 0 & 0 & -\frac{n(s)}{\rho(s)^2} & 0 & 0 & 0 \\ -\frac{1}{\rho(s)} & 0 & 0 & 0 & 0 & \frac{1}{\gamma^2} \\ 0 & 0 & 0 & 0 & 0 & 0 \end{pmatrix} \quad (13)$$

is the infinitesimal transfer matrix, and

$$\mathbf{X} = \begin{pmatrix} x \\ p_x \\ y \\ p_y \\ z \\ p_z \end{pmatrix} = \begin{pmatrix} x \\ x' \\ y \\ y' \\ z \\ \gamma^2 z' \end{pmatrix} \quad (14)$$

is the particle state vector.

## LINEAR OPTICS FROM GEOMETRY

The objective of this section is to derive the relation between the geometry of the closed orbits and the coefficients that appear in the Hamiltonian of Eq. (11).

Let's consider an ensemble of closed orbits given by:

$$r(a, \theta): \mathbb{R}^+ \times \mathbb{R} \rightarrow \mathbb{R}^+, \quad (15)$$

where  $\theta$  is the azimuth and  $a$  is an orbit scale factor. For the orbits to be closed,  $r$  must be periodic:

$$r(a, \theta + 2\pi/N) = r(a, \theta + 2\pi/N) \text{ with } N \in \mathbb{N}^*. \quad (16)$$

Let's also assume that for all  $a$  and  $\theta$ :

$$\frac{\partial r}{\partial a} > 0; \quad (17)$$

this will ensure that the closed orbits with different scale factor (i.e. corresponding to different energies) do not cross over. The infinitesimal length increment of the orbit is given by (see Fig. 1):

$$\frac{ds}{d\theta} = \sqrt{r^2 + \left(\frac{\partial r}{\partial \theta}\right)^2}, \quad (18)$$

which leads to the orbit circumference:

$$\mathcal{L}(a) = \int_0^{2\pi} \sqrt{r^2 + \left(\frac{\partial r}{\partial \theta}\right)^2} d\theta. \quad (19)$$

The isochronous condition sets the relation between the circumference of the orbit and the particle energy through:

$$\beta = \frac{\mathcal{L}(a)}{r_\infty} \quad (20)$$

where  $2\pi r_\infty$  is the circumference of the orbit of a particle travelling at the speed of light. The curvature of the orbit is given by:

$$\rho(a, \theta) = \frac{\left(r^2 + \left(\frac{\partial r}{\partial \theta}\right)^2\right)^{3/2}}{r^2 + 2\left(\frac{\partial r}{\partial \theta}\right)^2 - r\frac{\partial^2 r}{\partial \theta^2}}. \quad (21)$$

The field index writes, using Eqs. (5) and (9):

$$n = -\frac{q\rho^2}{P} \frac{\partial B}{\partial x} = \frac{\partial \rho}{\partial x} - \frac{\rho}{P} \frac{\partial P}{\partial x}. \quad (22)$$

Using the chain rule, and the relations between infinitesimal

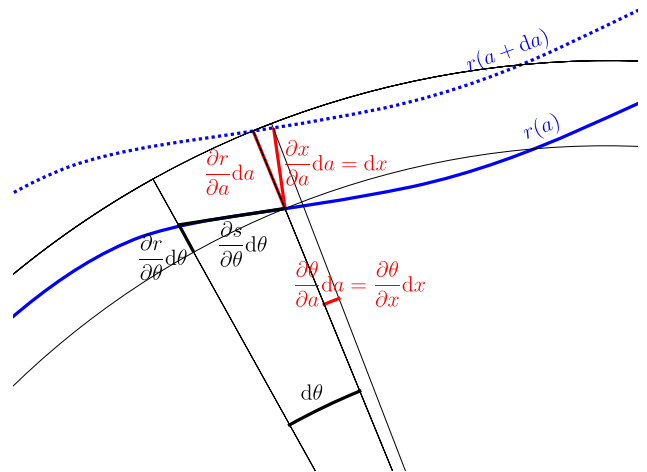


Figure 1: Relations between infinitesimal quantities around the closed orbit (the thick blue line);  $d\theta$  and  $da$  represent infinitesimal variations in  $\theta$  and  $a$  respectively.

quantities (see Fig. 1):

$$\frac{\partial \rho}{\partial x} = \frac{\partial \rho}{\partial a} \frac{\partial a}{\partial x} + \frac{\partial \rho}{\partial \theta} \frac{\partial \theta}{\partial x} = \frac{1}{r} \left( \frac{\partial \rho}{\partial a} \frac{ds}{d\theta} - \frac{\partial \rho}{\partial \theta} \frac{\partial r}{\partial a} \right), \quad (23)$$

where  $\frac{ds}{d\theta}$  is given by Eq. (18). Finally:

$$\frac{\partial P}{\partial x} = \frac{d\beta}{da} \frac{mc}{r(1-\beta^2)^{3/2}} \frac{ds}{d\theta}, \quad (24)$$

where  $\beta$  is given by Eq. (20). All the coefficients that appear in Eq. (11) are given by  $r$  and its partial derivatives:  $\rho$  from Eq. (21),  $\gamma$  from Eq. (20), and  $n$  from Eqs. (20) and (22) to (24).

Now that we know how to write linear-motion Hamiltonian explicitly, we can calculate the transverse tunes. This is done by numerically integrating a  $\theta$ -based version of Eq. (12):

$$\frac{d\mathbf{X}}{d\theta} = \mathbf{X}' \frac{ds}{d\theta} = \mathbf{F}\mathbf{X} \frac{ds}{d\theta} \quad (25)$$

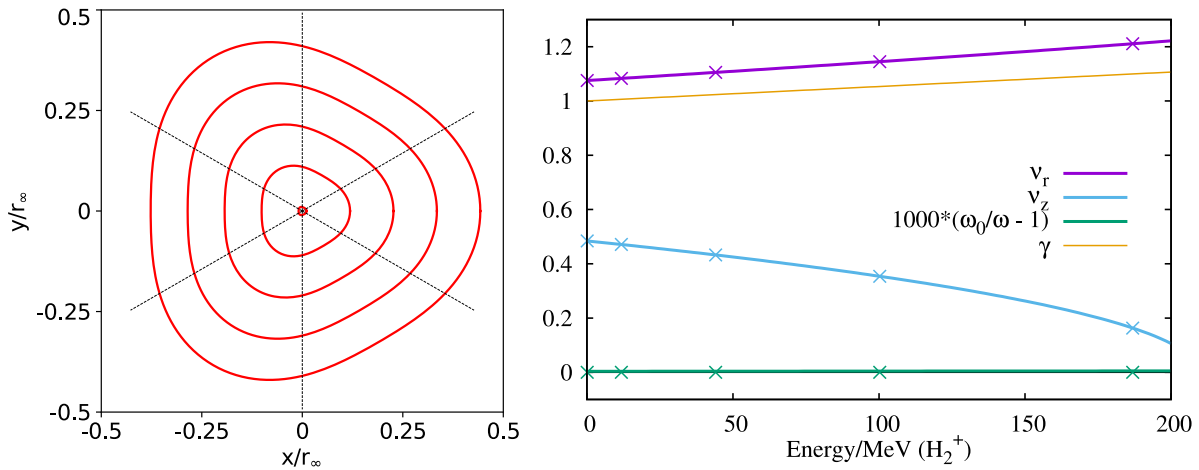


Figure 2: **Left:** the red lines represent 5 closed orbits with scale value  $a$  ranging between  $0.01 \times r_\infty$  and  $0.41 \times r_\infty$ ; the black dotted lines are lines of constant  $\phi$  value. **Right:** corresponding horizontal (purple) and vertical (blue) tune variation with energy; the green curve represents the relative variation of the revolution frequency; the orange line represents the Lorentz factor  $\gamma$ .

over one period for two different sets of initial transverse state vectors:  $\mathbf{X} = (1, 0, 1, 0, 0, 0)^T$  and  $\mathbf{X} = (0, 1, 0, 1, 0, 0)^T$ , see for instance Ref. [7].

To verify the tune calculated from numerical integration of Eq. (25), I also run CYCLOPS using 2-dimension field maps constructed by evaluating on a polar grid:

$$B(r, \theta) = \frac{\beta(a(r, \theta))}{\sqrt{1 - \beta^2(a(r, \theta))}} \frac{m}{q\rho(a(r, \theta), \theta)}, \quad (26)$$

where  $\rho(a, \theta)$  is given by Eq. (21),  $\beta(a)$  is given by Eq. (20).  $a(r, \theta)$  is calculated from  $r(a, \theta)$  using numerical root finding.

The source code used to calculate tunes and generate fields maps for all the examples presented below is available on: <https://gitlab.triumf.ca/tplanche/from-orbit>

## EXAMPLES

Let's now consider an ensemble of closed orbits written in the form of a truncated Fourier series:

$$r(a, \theta) = a [1 + C(a) \cos(N(\theta - \phi(a)))], \quad (27)$$

where  $N$  is the number of sectors.

Table 1: Examples of Orbit Shape Parameters. The names in the first row refer to the titles of the corresponding sub-sections.

$a/r_\infty$	Gordon		spiral		N=3 flat tunes		N=5 flat tunes	
	$C$	$\phi$	$C$	$\phi$	$C$	$\phi$	$C$	$\phi$
0.01	0.08	0	0	0	0	0	0	0
0.11	0.08	0	0.04	0.319	0.0885	0.531	0.0614	0.827
0.21	0.08	0	0.04	0.719	0.0980	0.513	0.0748	0.94
0.31	0.08	0	0.04	1.082	0.0882	0.362	0.0712	0.992
0.41	0.08	0	0.04	1.427	0.0632	0.147	0.0591	1.103

### 3-sector Soft-edge Gordon Cyclotron

The first example I propose to study is a soft-edge version of Gordon's radial-sector cyclotron [1]. I choose the number

of sectors  $N = 3$ , and  $C(a) = 0.08$  for all  $a$ . In other words, all closed orbits are photographic enlargements with no rotation, see Fig. 2.

$H_2^+$  is chosen as the injection particle to run the CYCLOPS. Results are presented in Fig. 2. Agreement between the calculation from geometry (crosses) and using a field map with CYCLOPS (solid lines) is perfect. As expected, the field is isochronous: the maximum relative deviation from isochronism calculated by CYCLOPS is of the order of  $10^{-5}$ . Note that the results presented in Fig. 2 are independent of the value chosen for  $r_\infty$ .

### 3-sector Spiral Cyclotron

In all the following examples I define  $C(a)$  and  $\phi(a)$  as cubic splines constrained at 5 knots ranging from  $a = 0.01 \times r_\infty$  to  $a = 0.41 \times r_\infty$ , see Table 1. I also impose the most central orbit to be circular, i.e.  $C(0.01 \times r_\infty) = 0$ . The intention is to account for the fact that closed orbits with a radius comparable with the magnetic gap are, in practice, very close to perfect circles.

For the second 3-sector example, I choose  $C = 0.04$  for the outer orbits. I use the 'minimize' function from SCIPY.OPTIMIZE to minimize the variation of the vertical tune by adjusting the value of  $\phi$  of the 4 outer orbits. The result is presented in Table 1 and Fig. 3. The agreement between the calculation from geometry and using a field map with CYCLOPS is again perfect, and the result is independent of the choice  $r_\infty$ .

### 3-sector Cyclotron with Flat Transverse Tunes

For the third 3-sector example, I let both  $C$  and  $\phi$  vary for the 4 outer orbits, with the objective to minimize the variation of both transverse tunes. The result is presented in Table 1 and Fig. 5. This example is not dissimilar to the one presented in Ref. [8], except that the relative variation of the revolution frequency is here of the order of  $10^{-5}$ .

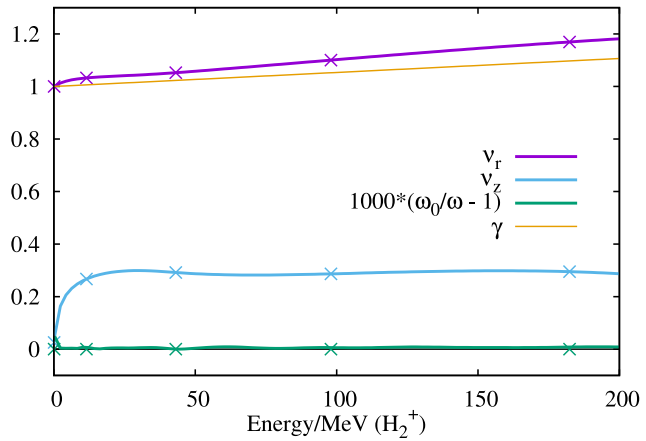
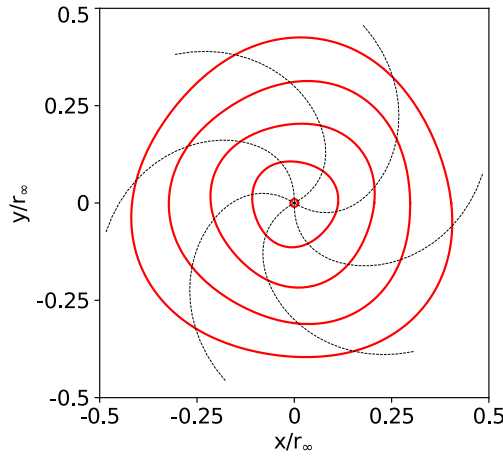


Figure 3: 3-sector spiral sector cyclotron example. Crosses show results calculated from the geometry of the orbits. The solid lines show results obtained using a field map and the computer code `CYCLOPS`. For a detailed plot description, please refer to the caption of Fig. 2.

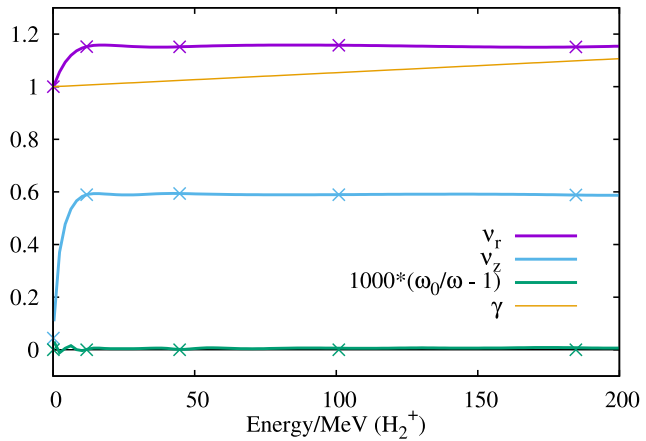
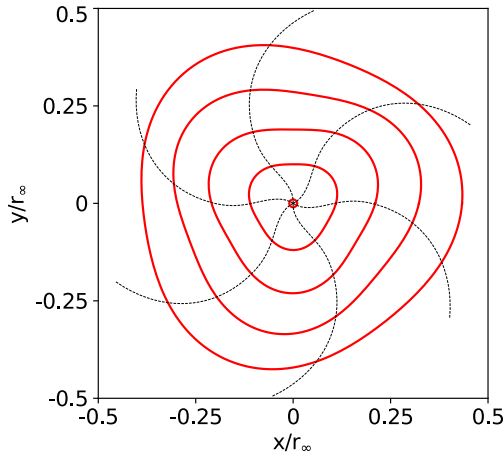


Figure 4: 3-sector spiral sector cyclotron example with stabilized radial tune. Crosses show results calculated from the geometry of the orbits. The solid lines show results obtained using a field map and the computer code `CYCLOPS`. For a detailed plot description, please refer to the caption of Fig. 2.

### 5-sector Cyclotron With Flat Transverse Tunes

The fourth example is a 5-sector version of the previous example. The result is presented in Table 1 and Fig. 5.

### SCALING FFA

One may, for instance, substitute the isochronous condition, that is Eq. (20), by the following scaling law [9]:

$$P(a) = P_0 \left( \frac{a}{a_0} \right)^{k+1} \quad (28)$$

where  $P$  is the momentum associated with the closed orbit;  $k$ ,  $P_0$ , and  $a_0$  are constants. If  $C(a)$  is kept constant, and  $\phi(a)$  is chosen to follow a logarithmic spiral [9]:

$$\phi(a) = \tan(\zeta) \ln \left( \frac{a}{a_0} \right), \quad (29)$$

the resulting machine is scaling fixed field accelerator (FFA). It is not isochronous<sup>2</sup> and may be called a synchro-cyclotron. In the particular case  $\zeta = 0$ , the machine has radial sectors.

<sup>2</sup> except immediately around the transition energy given by  $\gamma = \sqrt{k+1}$

As a scaling FFA example I choose  $N = 4$ ,  $C = 0.02$ ,  $k = 0.2$  and  $\zeta = 60$  degree. As expected the transverse tunes calculated using the geometrical parameters of the orbits are constant, see Fig. 6. Agreement with `CYCLOPS` is again perfect. These results have also been crosschecked using the analytic field model of the code `FIXFIELD` [10].

### CONCLUSION

I have described a method to generate fixed field distributions starting from the geometry of the closed orbits. This method is useful to rapidly produce isochronous field maps without the need for finite element calculations. Among the few isochronous examples presented in this paper, two have stabilized vertical and radial tunes. These two examples have in common their non-monotonic radial variation of the magnetic flutter and spiral angle.

### REFERENCES

- [1] M. Gordon, "Orbit properties of the isochronous cyclotron ring with radial sectors," *Annals of Physics*, vol. 50, no. 3, pp.

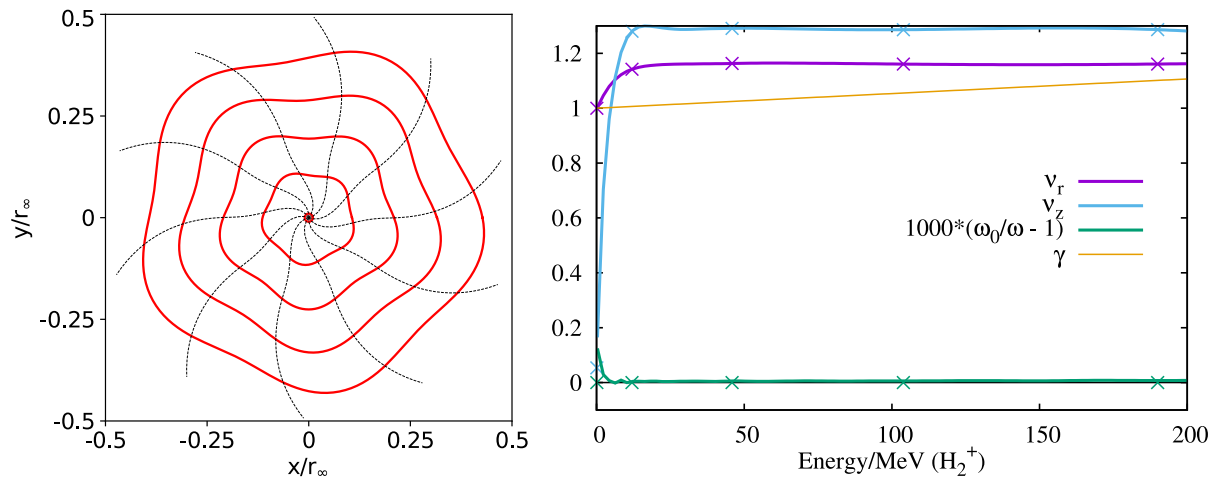


Figure 5: 5-sector cyclotron example. Crosses show results calculated from the geometry of the orbits. The solid lines show results obtained using a field map and the computer code CYCLOPS. For a detailed plot description, please refer to the caption of Fig. 2. Note the negative bends.

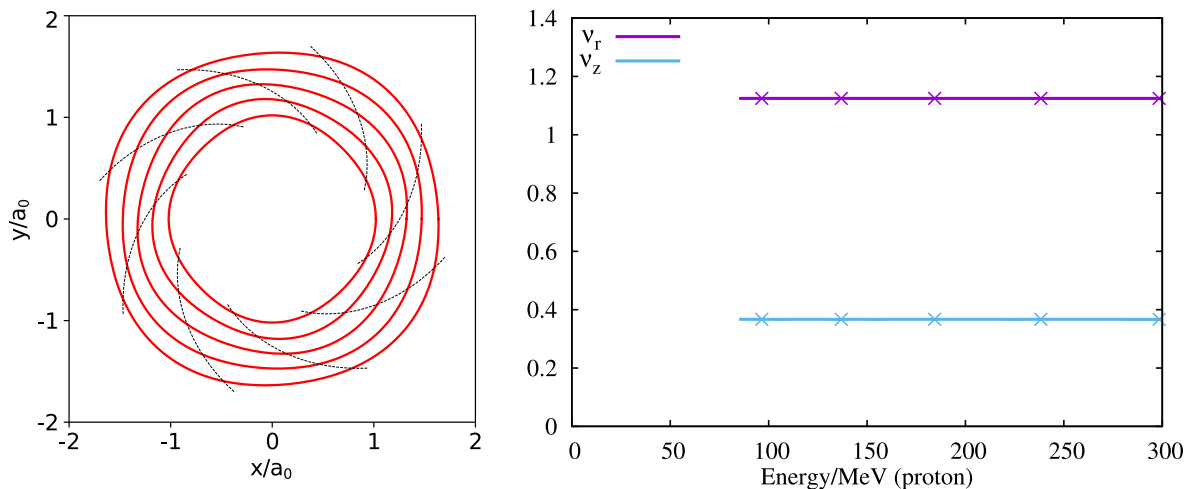


Figure 6: 4-sector spiral scaling FFA example. Crosses show results calculated from the geometry of the orbits. The solid lines show results obtained using a field map and the computer code CYCLOPS.

571–597, 1968. doi:10.1016/0003-4916(68)90132-2

[2] W. Joho, “Simulating cyclotron sector magnets with the computer program TRANSPORT,” TRIUMF, Tech. Rep. TRI-BN-82-12, 1982. <http://lin12.triumf.ca/text/2002FFAG/TRI-DN-82-12.PDF>

[3] J. Botman, “Ring cyclotrons with return field gullies,” TRIUMF, Tech. Rep. TRI-BN-82-20, 1982. <http://lin12.triumf.ca/text/2002FFAG/TRI-DN-82-20.PDF>

[4] M. Craddock and K. Symon, “Cyclotrons and fixed-field alternating-gradient accelerators,” *Rev. Accel. Sci. Technol.*, vol. 1, no. 01, pp. 65–97, 2008. doi:10.1142/9789812835215\_0004

[5] R. Baartman, “Linearized Equations of Motion in Magnet with Median Plane Symmetry,” TRIUMF, Tech. Rep. TRI-DN-05-06, 2005.

[6] E. Courant and H. Snyder, “Theory of the alternating-gradient synchrotron,” *Annals Phys.*, vol. 3, no. 1, pp. 1 – 48, 1958. doi:10.1016/0003-4916(58)90012-5

[7] C. Meade, “Changes to the main magnet code,” TRIUMF, Tech. Rep. TRI-DN-70-54-Addendum4, 1971. <http://lin12.triumf.ca/design-notes/1970/TRI-DN-70-54-Addendum4.PDF>

[8] D. Bruton *et al.*, “A compact and high current FFA for the production of radioisotopes for medical application”, in *Proc. IPAC’16*, Busan, Korea, 2016. doi:10.18429/JACoW-IPAC2016-TUPOY023

[9] K. R. Symon, D. W. Kerst, L. W. Jones, L. J. Laslett, and K. M. Terwilliger, “Fixed-field alternating-gradient particle accelerators,” *Phys. Rev.*, vol. 103, pp. 1837–1859, Sep 1956. doi:10.1103/PhysRev.103.1837

[10] J.-B. Lagrange, D. J. Kelliher, S. Machida, C. R. Prior, and C. T. Rogers, “Status of FFAs (Modelling and Existing/planned Machines)”, presented at the Cyclotrons’19, Cape Town, South Africa, Sep. 2019, paper WEB01.